Published in final edited form as:

Oncogene. 2016 August 18; 35(33): 4312–4320. doi:10.1038/onc.2015.492.

Hypoxia-upregulated microRNA-630 targets Dicer, leading to increased tumor progression

Rajesha Rupaimoole[1,2], **Cristina Ivan**[1,3], **Da Yang**[4], **Kshipra M. Gharpure**[1,2], **Sherry Y. Wu**[1], **Chad V. Pecot**[5], **Rebecca A. Previs**[1], **Archana S. Nagaraja**[1,2], **Guillermo N Armaiz-Pena**[1], **Michael McGuire**[1], **Sunila Pradeep**[1], **Lingegowda S. Mangala**[1,3], **Cristian Rodriguez-Aguayo**[3,6], **Li Huang**[7], **Menashe Bar-Eli**[7], **Wei Zhang**[8], **Gabriel Lopez-Berestein**[3,6], **George A. Calin**[3,6], and **Anil K. Sood**[1,3,7]

[1]Department of Gynecologic Oncology & Reproductive Medicine, The University of Texas MD Anderson Cancer Center, 1515 Holcombe Blvd, Houston, TX 77030, USA

[2]Graduate School of Biomedical Sciences, The University of Texas MD Anderson Cancer Center, 1515 Holcombe Blvd, Houston, TX 77030, USA

[3]Center for RNA Interference and Non-Coding RNA, The University of Texas MD Anderson Cancer Center, 1515 Holcombe Blvd, Houston, TX 77030, USA

[4]Department of Pharmaceutical Sciences, University of Pittsburgh, 633A Salk Hall, 3501 Terrace Street, Pittsburgh, PA 15261, USA

[5]Deaprtment of Medicine, University of North Carolina Lineberger Comprehensive Cancer Center, 101 Manning Drive, Chapel Hill, NC 27599, USA

[6]Department of Experimental Therapeutics, The University of Texas MD Anderson Cancer Center, 1515 Holcombe Blvd, Houston, TX 77030, USA

[7]Department of Cancer Biology, The University of Texas MD Anderson Cancer Center, 1515 Holcombe Blvd, Houston, TX 77030, USA

[8]Department of Pathology, The University of Texas MD Anderson Cancer Center, 1515 Holcombe Blvd, Houston, TX 77030, USA

Corresponding author: Anil K. Sood, MD, Professor, Department of Gynecologic Oncology & Reproductive Medicine and Cancer Biology, Center for RNA Interference and Non-Coding RNAs, The University of Texas MD Anderson Cancer Center, Houston, TX 77030, USA; asood@mdanderson.org; Phone: 713-745-5266.

Authors' Contributions:

Conception and design: R. Rupaimoole, A.K. Sood

Development of methodology: R. Rupaimoole, A.K. Sood

Acquisition of data (provided animals, acquired and managed patients, provided facilities, etc.): R. Rupaimoole, S. Y. Wu, C. V. Pecot, R. A. Previs, K. M. Gharpure, A. S. Nagaraja, G. N. Armaiz-Pena, M. McGuire, S. Pradeep, L. S. Mangala, C. Rodriguez-Aguayo, L. Huang, M. Bar-Eli, W. Zhang, G. Lopez-Berestein, G. A Calin, A. K. Sood

Analysis and interpretation of data (e.g., statistical analysis, biostatistics, computational analysis): C. Ivan, D. Yang

Writing, review, and/or revision of the manuscript: R. Rupaimoole, A. K. Sood

Administrative, technical, or material support (i.e., reporting or organizing data, constructing databases): R. Rupaimoole, A. K. Sood

Study supervision: R. Rupaimoole, A. K. Sood

Disclosure of Potential Conflicts of Interest: No conflict of interests disclosed by authors.

Abstract

MicroRNAs (miRNAs) are small RNA molecules that affect cellular processes by controlling gene expression. Recent studies have shown that hypoxia downregulates Drosha and Dicer, key enzymes in miRNA biogenesis, causing a decreased pool of miRNAs in cancer, and resulting in increased tumor growth and metastasis. Here, we demonstrate a previously unrecognized mechanism by which hypoxia downregulates Dicer. We found that miR-630, which is upregulated under hypoxic conditions, targets and downregulates Dicer expression. In an orthotopic mouse model of ovarian cancer, delivery of miR-630 using DOPC nanoliposomes resulted in increased tumor growth and metastasis and decreased Dicer expression. Treatment with the combination of anti-miR-630 and anti-vascular endothelial growth factor antibody in mice resulted in rescue of Dicer expression and significantly decreased tumor growth and metastasis. These results indicate that targeting miR-630 is a promising approach to overcome Dicer deregulation in cancer. As demonstrated in the study, use of DOPC nanoliposomes for anti-miR delivery serves as a better alternative approach to cell line based overexpression of sense or anti-sense miRNAs, while avoiding potential *in vitro* selection effects. Findings from this study provide a new understanding of miRNA biogenesis downregulation observed under hypoxia and suggest therapeutic avenues to target this dysregulation in cancer.

Keywords

miRNAs; Dicer; Hypoxia; miRNA-630; Metastasis

Introduction

MicroRNAs (miRNAs) are evolutionarily conserved small RNA molecules that are involved in gene regulation by targeting mRNA to suppress gene expression[3, 5, 13]. Dicer and Drosha, two key enzymes involved in miRNA biogenesis pathways, are downregulated in several types of cancer which is associated with poor patient survival[9, 16]. Recently, our group reported that decreased Drosha and Dicer levels lead to downregulation of miRNA biogenesis in cancer[22, 27]. In the current report, we show a novel mechanism by which miR-630, which is upregulated under hypoxic conditions, regulates Dicer expression by directly targeting the Dicer 3’ untranslated region (UTR). We demonstrate that miR-630 increases tumor growth and metastasis when delivered *via* a 1,2-dioleoyl-sn-glycero-3-phosphocholine (DOPC) nanoliposome miRNA delivery platform, which is currently being tested in clinical trials. When anti-vascular endothelial growth factor (VEGF) therapy (known to induce hypoxia) was combined with anti-miR-630 therapy, Dicer expression was rescued, leading to reduction in tumor growth and metastasis.

Results

Hypoxia-upregulated miR-630 targets Dicer

In a previous study, we reported that Drosha and Dicer are downregulated under hypoxic conditions, and ETS1/ELK1-mediated transcriptional repression is the mechanism of Drosha downregulation[22]. While investigating Dicer downregulation under hypoxia conditions, we observed a significant decrease in Dicer 3’UTR luciferase reporter activity in cells exposed

to hypoxia (Figure 1A, Supp. Figure 1A). The decrease in 3'UTR activity prompted us to examine whether miRNAs are responsible for Dicer regulation under hypoxic conditions. To determine the specific miRNAs that are potentially involved in the downregulation of Dicer, we performed an integrative analysis using publicly available miRNA target prediction software and a miRNA array[22] that compares miRNA expression under normoxic and hypoxic conditions. From the array of upregulated miRNAs, we identified 10 miRNAs that have potential miRNA target sites in the 3'UTR of Dicer (Figure 1B). To validate these findings, we performed quantitative real-time polymerase chain reaction (PCR) with these upregulated miRNAs from the miRNA microarray, and 8 miRNAs showed significantly increased expression in A2780 ovarian cancer cells exposed to hypoxia (Figure 1C).

We subsequently transfected these 8 miRNA mimics into A2780 cells. Only miR-630 resulted in a decrease in Dicer mRNA and protein expression (Figure 1D, Supp. Figure 1B), indicating a potential role for miR-630 in targeting Dicer. We tested upregulation of miR-630 in additional cell lines, including the ovarian cancer cell line OVCAR3 and the breast cancer cell line MCF7. In both cell types, we observed consistent increases in miR-630 expression after exposure to hypoxia (Supp. Figure 1C). Upon transfecting anti-miR-630 into cells exposed to hypoxia, we observed significant rescue of Dicer expression (Figure 1D, Supp. Figure 1D).

To determine the definitive role of miR-630–mediated downregulation of Dicer, we performed a Dicer 3'UTR assay with mutated 3' UTR miR-630 binding site with or without transfection of miR-630. Data showed a significant reduction in luciferase reporter activity in cells treated with miR-630 compared with cells treated with control miRNA in wild type 3" UTR cells (Figure 1E, Supp. Figure 1E). In cells with a mutation in the Dicer 3'UTR region that corresponds to the miR-630 binding region, the effect of miR-630 on Dicer 3'UTR luciferase reporter activity after transfection with the miR-630 mimic was abrogated (Figure 1E, Supp. Figure 1E).

Quantification of precursor miR-630 showed increased expression of pri-miR-630 under hypoxic conditions, suggesting that miR-630 is transcriptionally upregulated (Supp. Figure 2A). Deep sequencing mRNA data A2780 from cells treated with hypoxia[22] were cross-referenced with the miR-630 promoter analysis to potentially identify transcription factors that could regulate miR-630 expression. STAT1 was identified as a transcription factor that binds directly to the promoter region of miR-630 (Supp. Figure 2B) and potentially leads to increased precursor levels of miR-630. Under hypoxic conditions, phospo-STAT1 levels were increased significantly at the mRNA and protein levels (Supp. Figure 2C). Use of siRNA-mediated gene silencing led to significant STAT1 gene knockdown (Supp. Figure 2D). Expression of miR-630 was significantly reduced under hypoxic conditions when cells were treated with siSTAT1 (Supp. Figure 2E), and a corresponding rescue in Dicer expression levels (Supp. Figure 2F) was also observed. Upon chromatin hybridization and immunoprecipitation (ChIP) assay with STAT1 antibody, we observed significant binding of STAT1 to miR-630 promoter region. RNA polymerase II ChIP was used as a positive control (Supp. Figure 2G).

MiR-630 expression correlates with hypoxia in vivo and in ovarian cancer clinical samples

Consistent with our *in vitro* findings, we observed a substantial increase in both precursor and mature miR-630 expression levels in tumor samples from the A2780 *in vivo* model in which mice had been treated with a VEGF-targeted antibody (bevacizumab) known to result in profound hypoxia in the tumor microenvironment (Figure 2A–B). Next, we examined 30 human epithelial ovarian cancer samples with known hypoxia profile (15 with high- and 15 with low levels of hypoxia)[22]. Data analysis showed a significant positive correlation between expression levels of miR-630 and the hypoxia marker CA9 (Figure 2C). In addition, we observed a significant negative correlation between miR-630 expression and Dicer levels in these clinical samples (Figure 2D).

Next, we interrogated The Cancer Genome Atlas (TCGA) dataset for high grade serous ovarian cancer to further investigate the correlation between expression of miR-630 and hypoxia-upregulated miR-210, a hypoxia marker. We observed a significant positive correlation between these 2 miRNAs (Figure 2E). We next examined the survival difference between patients with high and low miR-630 levels in their tumors using the ovarian cancer dataset from TCGA. We observed significantly worse overall survival rates in patients whose tumors had high levels of miR-630 (Figure 2F). We also examined expression of miR-630 using *in situ* hybridization and CA9 using immunofluorescence in ovarian tumor samples (Figure 2G). Microscopically, sections showed co-localization of areas with high miR-630 expression in highly hypoxic areas.

MiR-630–mediated Dicer downregulation under hypoxic conditions leads to tumor growth in vivo

Previously, we have shown decreases in Dicer and Drosha levels under hypoxic conditions, resulting in increased tumor progression *via* enhanced epithelial-to-mesenchymal transition (EMT). In this context, we tested the phenotypic effect of miR-630 downregulation in cells under normoxic and hypoxic conditions. When miR-630 was transfected into cells under normoxic conditions, cells showed significant increases in migration and invasion (Figure 3A–B). Inhibiting miR-630 under hypoxic conditions led to increased Dicer expression and a significant decrease in migration and invasion (Figure 3A–B).

We also analyzed expression of E-cadherin and vimentin, two EMT markers, after introducing miR-630 under normoxic conditions or anti-miR-630 under hypoxic conditions. Data showed significant induction of EMT upon introduction of miR-630 under normoxic conditions, and this effect was reversed by treatment with anti-miR-630 under hypoxic conditions (Figure 3C).

To understand the biological implications of miR-630–mediated Dicer downregulation under hypoxic conditions, we delivered miR-630 incorporated in DOPC nanoliposomes to A2780 tumor-bearing mice. There was a significant increase in tumor weight and distant metastases following treatment with miR-630-DOPC (Figure 3D–H). Interestingly, rare metastases such as lung metastases were observed in the miR-630 treatment group (Figure 3G, dotted circle). We also observed metastases in other sites, including the omentum and the liver, in the miR-630 treatment group, whereas minimal metastases were observed in the control group

(Figure 3H). Decreased Dicer RNA and protein expression was observed in tumors from mice treated with miR-630 (Figure 3I).

We next sought to explore combinations of anti-miR-630 and anti-VEGF therapy. Mice were treated with bevacizumab after tumor establishment, and we observed a significant increase in tumor weight and the number of metastatic nodules in the bevacizumab treatment group (Figure 4A–D). In mice treated with anti-miR-630 in addition to bevacizumab, we observed significant reductions in tumor weight and the number of metastatic nodules compared with mice treated with bevacizumab alone (Figure 4A–D). A significant reduction in metastatic spread was observed in the anti-miR-630 treatment group compared with the control group (Figure 4D). In addition, a significant increase in CA9 expression was observed in mice that received anti-VEGF therapy compared with control mice (Figure 4E). Importantly, we noted rescue of Dicer expression in the anti-miR-630 treatment group (Figure 4F).

Discussion

Here, we show a previously unrecognized mechanism by which hypoxia downregulates Dicer, a key enzyme in miRNA biogenesis. We provide evidence that miR-630, which is transcriptionally upregulated under hypoxic conditions, targets and decreases Dicer expression. In an orthotopic mouse model of ovarian cancer, delivery of miR-630 using DOPC nanoparticles resulted in increased tumor growth and metastasis and decreased Dicer expression. Treatment with the combination of anti-VEGF and anti-miR-630 in the mice resulted in rescue of Dicer expression and significantly decreased tumor growth and metastasis.

During progression, tumor cells encounter significant hypoxia owing to abnormal vasculature[7]. Emerging studies have shown that hypoxia is involved in promoting tumor progression and resistance to therapy[7, 23]. Direct assessment of tumor hypoxia in patient samples has demonstrated worse clinical outcomes in patients whose tumors had high levels of hypoxia[28]. In addition, emerging data suggest that anti-VEGF therapies in current clinical use induce significant hypoxia in tumors[14, 31]. We observed that short-term anti-VEGF therapy results in potential “angiogenesis rebound,” resulting in increased cancer growth and metastasis[22].

Global downregulation of miRNAs under hypoxic conditions has been reported. However, thus far, studies have shown that only a few miRNAs are upregulated under hypoxic conditions, and most of these are not well characterized. One of the well-studied miRNAs that is upregulated under hypoxic conditions is miR-210, a transcriptional target of HIF1-α[8, 10]. Target analysis has shown that miR-210 downregulates SDHD, leading to stabilization of HIF1-α[21] and an apoptosis-inducing factor called mitochondrion-associated 3 (AIFM3), known to induce cell death[17].

In the current study, we report a novel role of miR-630, which is also upregulated under hypoxic conditions. Previously, miR-630 was shown to modulate apoptosis in cells treated with cisplatin by decreasing DNA damage and promoting cell survival[6]. However, the mechanism by which this occurs has not been identified. Another recent study showed that

miR-630 targets SLUG, resulting in reduced invasion[11]. Our study significantly broadens the understanding of how miR-630 can enhance tumor metastasis, suggesting distinctive role of miR-630 in cells under exposure to hypoxia. Through several lines of evidence, we showed that miR-630 is able to target Dicer and is responsible for hypoxia-mediated tumor progression and metastasis. Even though we observed significant reduction in metastasis upon treatment with anti-miR-630 compared to anti-VEGF therapy alone, these effects could be driven by additional genes, which are rescued by anti-miR-630 and require further investigation. Hypoxia signaling involves multiple cell types within tumor microenvironment and the effect of anti-miR-630 on these cells such as endothelial cells remain to be investigated.

We and others have shown that decreased expression of Drosha and Dicer in cancer is associated with poor clinical outcomes[4, 9, 16, 24, 25]. Mechanisms for Drosha downregulation include transcriptional downregulation via c-myc[29] and ADARB1[1]. For Dicer, direct binding of *Tap63* transcription factor to the Dicer promoter has been shown to downregulate Dicer, as has loss of TAp63 in cancer[25]. Two independent studies have shown different miRNAs targeting Dicer, specifically miR-103/107[15] and let-7[26]. Previously, we reported that a significant number of miRNAs were affected by hypoxia-mediated Dicer downregulation, and we showed the mechanism by which this downregulation leads to increased tumor progression[22, 27]. In these studies, we reported that Dicer is downregulated in breast cancer cells exposed to hypoxia via an epigenetic mechanism involving oxygen deprivation–mediated inhibition of KDM6A/B, a demethylase enzyme. However, understanding of Dicer downregulation in cancer has thus far been limited to a few studies showing involvement of specific miRNAs such as let7 and miR-103/107 or transcriptional regulation by TAp63[15, 25, 26]. These studies do not consider the influence of the tumor microenvironment on Dicer downregulation. In contrast, we show in the current report that hypoxia-induced downregulation of miRNA biogenesis is a highly dynamic process[22, 27]. Our study not only sheds light on the mechanism by which hypoxia regulates Dicer, but also suggests that miRNA/RNAi-based gene targeting may be a useful strategy to develop therapies targeting genes that cannot be treated using classic chemical agents or antibodies[18–20]. As demonstrated in our study, the DOPC liposome-anti-miRNA system for *in vivo* delivery acts as a promising therapeutic approach to rescue the expression of Dicer in cancer.

In summary, our study provides a clear mechanistic link between hypoxia and tumor progression *via* upregulation of miR-630 and downregulation of Dicer. These findings could translate into the development of new therapeutic approaches that target deregulated miRNA biogenesis in cancer.

Methods

Cell line maintenance and siRNA and miRNA transfections

All cancer cell lines were maintained at 37°C in 5% CO_2. Ovarian cancer (A2780 and OVCAR3) and breast cancer (MCF7) cancer cell lines were obtained from the American Type Culture Collection. Cells and were maintained in culture with RPMI-1640 supplemented with 10–15% fetal bovine serum (FBS) and 0.1% gentamicin sulfate (Gemini Bioproducts, Calabasas, CA). Cell lines were tested routinely to confirm the absence of

mycoplasma, and *in vitro* experiments were conducted with cultures at 60–80% confluence. All siRNA transfections were performed using RNAiMAX (Invitrogen, Carlsbad, CA) reagent following the forward transfection protocol from the manufacturer. To minimize toxicity, media was changed five hours after transfections. For hypoxia treatments, cells were incubated in an oxygen-controlled hypoxia chamber at 1% O_2. Sequences for siRNAs are as follows: siDicer1 S 5' CAUUGAUCCUGUCAUGGAU [dT] [dT] 3' AS 5' AUCCAUGACAGGAUCAAUG [dT] [dT] 3' siDicer2 S 5' GCAGUUAUGAUUUAGCUAA [dT] [dT] 3' AS 5' UUAGCUAAAUCAUAACUGC [dT] [dT] 3', siSTAT1-1 1 S 5' CUCAUUCCGUGGACGAGGU [dT] [dT] 3' AS 5' ACCUCGUCCACGGAAUGAG [dT] [dT] 3' siSTAT1-2 S 5' CCUGAUUAAUGAUGAACUA [dT] [dT] 3' AS 5' UAGUUCAUCAUUAAUCAGG [dT] [dT] 3'.

In vivo models

Female athymic nude mice were purchased from Taconic Farms (Hudson, NY). Animals were cared for according to guidelines set forth by the American Association for Accreditation of Laboratory Animal Care and the US Public Health Service policy on Human Care and Use of Laboratory Animals. Mouse studies were approved and supervised by The University of Texas MD Anderson Cancer Center Institutional Animal Care and Use Committee. At the time of injection, all animals were 8–12 weeks old.

Orthotopic models of ovarian cancer were developed as described previously[2, 30]. For all animal experiments, cells were harvested using trypsin-EDTA, neutralized with FBS-containing media, washed, and resuspended to the appropriate cell number in Hanks' balanced salt solution (HBSS; Gibco, Carlsbad, CA) prior to injection. A2780 cells were directly injected into the ovary (0.8×10^6 cells in a 1:1 mixture of BD Matrigel and HBSS with a total volume of 100 μL of HBSS). For the intra-ovarian injections, mice were anesthetized with ketamine and xylazine. A small skin incison was made incision and dissection performed to visualize the right ovary. A 1-mL tuberculin syringe with a 30-gauge needle was used to inject the cell suspension directly into the ovary. Incisions were closed with surgical clips, and the mouse was returned to a cage until fully recovered. For all therapeutic experiments, a dose of 200 μg miRNA/kg was used, as described previously[12, 20, 30]. Twice weekly treatments via intraperitoneal injections commenced one week after cell inoculation and continued for four weeks. Mice were randomized and treated with miRNA incorporated in neutral DOPC nanoliposomes (intraperitoneal administration). Control groups received scrambled miRNA controls of same quantity. For the anti-VEGF therapy experiment, mice were allowed to develop tumors for two to three weeks, and twice weekly treatments with bevacizumab (6.25 mg/kg) were administered via intraperitoneal administration. For all experiments, once a mouse in any group became moribund, all groups were sacrificed, necropsied, and tumors were harvested. Tumor weight, number, and location of tumor nodules were recorded. Tumor tissue was either fixed in formalin for paraffin embedding, frozen in optimal cutting temperature media, or snap-frozen.

Liposomal nanoparticle preparation

MiRNA for *in vivo* delivery was incorporated into DOPC, as previously described[12]. DOPC and miRNA were mixed in the presence of excess tertiary butanol at a ratio of 1:10 (w/w) miRNA. Tween-20 was added in a ratio of 1:19. The mixture was vortexed, frozen in an acetone/dry ice bath, and lyophilized. Before *in vivo* administration, preparations were hydrated with phosphate-buffered saline at room temperature for a concentration of 200 μg miRNA per injection.

Tumor samples

Patient tumor samples were obtained as per the previously approved protocol[16]. We obtained 75 specimens of invasive epithelial ovarian cancer from The University of Texas MD Anderson Cancer Center Tumor Bank. For use as normal control, 15 benign ovarian epithelial samples were also obtained. Frozen tumor samples (approximately 0.2 mg each) were used for RNA isolation.

TCGA data and bioinformatics analysis

Agilent 44K gene expression, Agilent human miRNA microarray 8×15K miRNA expression data, and clinical information were obtained from the open access and controlled-access tiers of the TCGA data portal with NIH approval. Alignment of sample identifiers yielded 456 tumor cases with all information available at the time of data retrieval from the TCGA. Pearson correlation test, Kaplan-Meier, and Mantel-Cox survival analyses were performed using R 2.10.0. Significance was defined as $p < 0.05$.

Target gene binding sites, luciferase reporter assays, and Dicer 3'UTR site mutagenesis

The putative miRNA binding sites on Dicer 3'UTR were predicted bioinformatically using several algorithms for predicting miRNA targets. This was done using the following publicly available sites: http://www.microrna.org for the miRanda algorithm, http://www.targetscan.org for the TargetScan algorithm, http://genie.weizmann.ac.il/pubs/mir07 for the PITA algorithm, http://cbcsrv.watson.ibm.com for the RNA22 algorithm, http://diana.cslab.ece.ntua.gr/microT for the microT algorithm, and http://genome.ucsc.edu/cgi-bin/hgTables?command=start with http://pictar.mdc-berlin.de/ for the PicTar algorithm. The predicted miRNAs were shortlisted by cross-referencing miRNA data from the miRNA array (GSE52744). GoClone pLightSwitch luciferase reporters for the 3'UTR regions of Dicer were obtained from SwitchGear Genomics (Menlo Park, CA).

A2780 and MCF7 cells were transfected with FuGENE HD TFX reagent in a 96-well plate with scrambled control and miR-630 mimics (100nM; Ambion) along with the 3'UTR reporter gene and Cypridina TK control construct (pTK-Cluc). After 24 hours of transfection, luciferase activity was obtained with the LightSwitch Dual Luciferase assay kits using a microplate luminometer per manufacturer guidelines (Biotek). Luciferase activity was normalized using the Cypridina TK control construct, and an empty luciferase reporter vector was used as a negative control. The ratios obtained were further normalized according to the scrambled control. Mutants of the Dicer 3'UTR were generated using the QuikChange Lightning Multi Site-direct Mutagenesis kit (Agilent Technologies), using the primers (F

5’TGATGCAGATAAAGCAGGAAGGACCTCGGGTAAATGTCACTTACATATAAATGC AGCATTCCACGAAGCATCAAGTT3’) to mutate five base pairs within the miR-630 binding site. Mutagenesis was confirmed using Sanger DNA sequencing prior to luciferase assays.

Immunoblotting

Protein lysates from cultured cells were prepared using modified RIPA buffer (50mM Tris-HCl [pH 7.4], 150mM NaCl, 1% Triton, 0.5% deoxycholate) plus 25 μg/mL leupeptin, 10 μg/mL aprotinin, 2 mM EDTA, and 1 mM sodium orthovandate. Protein concentrations were determined using a BCA Protein Assay Reagent kit (Pierce Biotechnology, Rockford, IL). Lysates were loaded and separated on sodium dodecyl sulfate–polyacrylamide gels. Using semidry electrophoresis, proteins were transferred overnight to a nitrocellulose membrane, (Bio-Rad Laboratories, Hercules, CA) blocked with 5% bovine serum albumin for one hour, and incubated at 4°C overnight with primary antibody (Dicer [Novus Biologicals, Littleton, Colorado], STAT1, and pSTAT1 [Cell Signalling, Danvers, MA]). After washing with tris-buffered saline with Tween-20, membranes were incubated with horseradish peroxidase (HRP)–conjugated horse anti-mouse or rabbit IgG (1:2000; GE Healthcare) for two hours. Visualized of HRP was achieved by using an enhanced chemiluminescence detection kit (Pierce Biotechnology). To confirm equal loading of samples, blots were probed with an antibody specific for β-actin (0.1 μg/mL; Sigma)

Chromatin hybridization and immunoprecipitation assay

Cells were cultured in hypoxic or normoxic conditions for 48 h and chromatin immunoprecipitation assays were performed using the Chip-it express kit (Active Motif), as described by the manufacturer. In brief, cross-linked cells were collected, lysed, sonicated and subjected to immunoprecipitation with the STAT1, RNA Pol II antibodies or IgG isotype control. Immunocomplexes were collected with protein A/G agarose magnetic beads and eluted. Cross-links were reversed by incubation at 65 °C with high salt concentration. PCR-based quantification of percentage of input STAT1 binding on the miR-630 promoter region was performed. The 3,000 base upstream region of the STAT1 binding region was used as a control.

Quantitative real-time PCR

Total RNA was isolated using the Qiagen RNeasy kit (Qiagen). For miRNA quantification, total RNA was isolated using the Trizol/isopropanol total RNA precipitation method. Using 1000 ng of RNA, cDNA was synthesized using a Verso cDNA kit (Thermo Scientific), as per manufacturer instructions. Analysis of mRNA levels was performed on a 7500 Fast Real-Time PCR System (Applied Biosystems) with SYBR Green-based real-time PCR for all genes. Dicer and Drosha Taqman assays (Life Technologies) were performed. Semi-quantitative real-time PCR was done with reverse-transcribed RNA and 100 ng/μL sense and antisense primers in a total volume of 20 μL. Total RNA was isolated using Trizol (Invitrogen) extraction. For pri-miRNA and mature miRNA quantifications, Taqman miRNA assays (Life Technologies) were used and reverse-transcription real-time PCR was performed, according to the manufacturer’s instructions. RNU6B (for mature miRNAs) or 18S (pri- and precursor miRNAs) were used as housekeeping genes. Primer sequences are as

follows: 18S: F 5'CGCCGCTAGAGGTGAAATTC3' R 5'TTGGCAAATGCTTTCGCTC3', STAT1: F 5'TGAATATTCCCCGACTGAGC3' R 5'AGGAAGACCCAATCCAGATGT3', miR630 ChIP: F 5'TGTGCCTTATTCACTGTTCCC3' R 5'TGGGCTCATTCACAGTTCCC3', Negative control ChIP: F 5' TCTTCCAAGCAGCCCTAAAG3' R 5' CAAGCATGGCCCTGTTATAC3'.

Migration and invasion assays

Modified Boyden chambers (Coster, Boston, MA) coated with 0.1% gelatin (migration) or extracellular matrix components (invasion) were used. A2780 cells (1×10^5) suspended in 100 μL of serum-free media were added into the upper chamber 24 hours after miRNA/siRNA transfections. Complete media containing 10% FBS (500 μL) was added to the bottom chamber as a chemo-attractant for cells. Chambers were incubated at 37°C in 5% CO_2 for six hours (migration) or overnight (invasion). After incubation, cells in the upper chamber were removed with cotton swabs. Cells were fixed and stained and counted using light microscopy. Cells from five random fields were counted.

In situ hybridization and immunofluorescence staining

Deparrafinization and rehydration of the formalin-fixed, paraffin-embedded tissue sections used xylene and an ethanol dilution series. Sections of tissue sections were digested with 15 μg/mL proteinase K for 20 minutes at room temperature and loaded onto Ventana Discovery Ultra for *in situ* hybridization analysis. Tissue slides were incubated with double-DIG labeled mercury LNA microRNA probe (exiqon) for two hours at 55°C. Three percent H_2O_2 was used to inactivate endogenous peroxidases. Following polyclonal anti-DIG antibody and HRP-conjugated secondary antibody (Ventana) incubation, tyramine-conjugated fluorochrome (TSA) reaction was performed for twelve minutes. Sequential TSA rounds were performed for the detection of proteins using the same protocol. Slides were mounted with antifading ProLong Gold Solution (Life Technologies).

Statistical analyses

Microsoft Excel or GraphPad Prism was used to analyze data. Continuous variables were compared using the Student's t-test or analysis of variance, and the Mann–Whitney test was used to compare differences. Using two-way analysis of variance, we determined that a sample size of 10 animals per group would provide an effective size of 1.3 with 80% power at a significance level of $P=0.05$. We considered $P<0.05$ to be statistically significant. All statistical analyses were expressed as mean±standard error of the mean.

Supplementary Material

Refer to Web version on PubMed Central for supplementary material.

Acknowledgements

Portions of this work were supported by the National Institutes of Health (P30 CA016672, CA109298, UH2TR000943-01, P50 CA083639, P50 CA098258, CA128797, RC2GM092599, U54 CA151668, and U24CA143835); the Cancer Prevention and Research Institute of Texas (RP110595); the Ovarian Cancer Research Fund, Inc. (Program Project Development Grant); the United States Department of Defense (OC073399, W81XWH-10-1-0158, and BC085265); the Marcus Foundation; the Red and Charline McCombs Institute for the

Early Detection and Treatment of Cancer; the RGK Foundation; the Gilder Foundation; the Estate of C.G. Johnson, Jr.; the Blanton-Davis Ovarian Cancer Research Program; and the Betty Anne Asche Murray Distinguished Professorship (A.K.S.). R.R. is supported in part by the Russell and Diana Hawkins Family Foundation Discovery Fellowship. S.Y.W. is supported by the Ovarian Cancer Research Fund, Inc., Foundation for Women's Cancer, and Cancer Prevention and Research Institute of Texas training grants (RP101502 and RP101489). R.A.P. is supported by the NCI-DHHS-NIH T32 training grant (T32 CA101642). C.V.P. was supported by a grant from the NCI (T32 training grant CA009666), the 2011 Conquer Cancer Foundation ASCO Young Investigator Award, and the DoCM Advanced Scholar Program. A.S.N. is supported by a Research Training Award from the Cancer Prevention and Research Institute of Texas (CPRIT RP140106). K.M.G. is supported by Altman Goldstein Discovery fellowship. The authors thank Dr. Xinna Zhang for assistance with the In-Situ hybridization analysis.

References

1. Allegra D, Bilan V, Garding A, Dohner H, Stilgenbauer S, Kuchenbauer F, et al. Defective DROSHA processing contributes to downregulation of MiR-15/-16 in chronic lymphocytic leukemia. Leukemia. 2014; 28:98–107. [PubMed: 23974981]
2. Armaiz-Pena GN, Allen JK, Cruz A, Stone RL, Nick AM, Lin YG, et al. Src activation by beta-adrenoreceptors is a key switch for tumour metastasis. Nature communications. 2013; 4:1403.
3. Bartel DP. MicroRNAs: genomics, biogenesis, mechanism, and function. Cell. 2004; 116:281–297. [PubMed: 14744438]
4. Dedes KJ, Natrajan R, Lambros MB, Geyer FC, Lopez-Garcia MA, Savage K, et al. Down-regulation of the miRNA master regulators Drosha and Dicer is associated with specific subgroups of breast cancer. European journal of cancer. 2011; 47:138–150. [PubMed: 20832293]
5. Esteller M. Non-coding RNAs in human disease. Nature reviews Genetics. 2011; 12:861–874.
6. Galluzzi L, Morselli E, Vitale I, Kepp O, Senovilla L, Criollo A, et al. miR-181a and miR-630 regulate cisplatin-induced cancer cell death. Cancer research. 2010; 70:1793–1803. [PubMed: 20145152]
7. Harris AL. Hypoxia--a key regulatory factor in tumour growth. Nature reviews Cancer. 2002; 2:38–47. [PubMed: 11902584]
8. Huang X, Ding L, Bennewith KL, Tong RT, Welford SM, Ang KK, et al. Hypoxia-inducible mir-210 regulates normoxic gene expression involved in tumor initiation. Molecular cell. 2009; 35:856–867. [PubMed: 19782034]
9. Karube Y, Tanaka H, Osada H, Tomida S, Tatematsu Y, Yanagisawa K, et al. Reduced expression of Dicer associated with poor prognosis in lung cancer patients. Cancer science. 2005; 96:111–115. [PubMed: 15723655]
10. Kulshreshtha R, Ferracin M, Wojcik SE, Garzon R, Alder H, Agosto-Perez FJ, et al. A microRNA signature of hypoxia. Molecular and cellular biology. 2007; 27:1859–1867. [PubMed: 17194750]
11. Kuo TC, Tan CT, Chang YW, Hong CC, Lee WJ, Chen MW, et al. Angiopoietin-like protein 1 suppresses SLUG to inhibit cancer cell motility. The Journal of clinical investigation. 2013; 123:1082–1095. [PubMed: 23434592]
12. Landen CN Jr, Chavez-Reyes A, Bucana C, Schmandt R, Deavers MT, Lopez-Berestein G, et al. Therapeutic EphA2 gene targeting in vivo using neutral liposomal small interfering RNA delivery. Cancer research. 2005; 65:6910–6918. [PubMed: 16061675]
13. Lee YS, Dutta A. MicroRNAs in cancer. Annual review of pathology. 2009; 4:199–227.
14. Mancuso MR, Davis R, Norberg SM, O'Brien S, Sennino B, Nakahara T, et al. Rapid vascular regrowth in tumors after reversal of VEGF inhibition. The Journal of clinical investigation. 2006; 116:2610–2621. [PubMed: 17016557]
15. Martello G, Rosato A, Ferrari F, Manfrin A, Cordenonsi M, Dupont S, et al. A MicroRNA targeting dicer for metastasis control. Cell. 2010; 141:1195–1207. [PubMed: 20603000]
16. Merritt WM, Lin YG, Han LY, Kamat AA, Spannuth WA, Schmandt R, et al. Dicer, Drosha, and outcomes in patients with ovarian cancer. The New England journal of medicine. 2008; 359:2641–2650. [PubMed: 19092150]
17. Mutharasan RK, Nagpal V, Ichikawa Y, Ardehali H. microRNA-210 is upregulated in hypoxic cardiomyocytes through Akt- and p53-dependent pathways and exerts cytoprotective effects.

American journal of physiology Heart and circulatory physiology. 2011; 301:H1519–H1530. [PubMed: 21841015]

18. Nishimura M, Jung EJ, Shah MY, Lu C, Spizzo R, Shimizu M, et al. Therapeutic synergy between microRNA and siRNA in ovarian cancer treatment. Cancer discovery. 2013
19. Pecot CV, Calin GA, Coleman RL, Lopez-Berestein G, Sood AK. RNA interference in the clinic: challenges and future directions. Nature reviews Cancer. 2011; 11:59–67. [PubMed: 21160526]
20. Pecot CV, Rupaimoole R, Yang D, Akbani R, Ivan C, Lu C, et al. Tumour angiogenesis regulation by the miR-200 family. Nature communications. 2013; 4:2427.
21. Puissegur MP, Mazure NM, Bertero T, Pradelli L, Grosso S, Robbe-Sermesant K, et al. miR-210 is overexpressed in late stages of lung cancer and mediates mitochondrial alterations associated with modulation of HIF-1 activity. Cell death and differentiation. 2011; 18:465–478. [PubMed: 20885442]
22. Rupaimoole R, Wu SY, Pradeep S, Ivan C, Pecot CV, Gharpure KM, et al. Hypoxia-mediated downregulation of miRNA biogenesis promotes tumour progression. Nature communications. 2014; 5:5202.
23. Shannon AM, Bouchier-Hayes DJ, Condron CM, Toomey D. Tumour hypoxia, chemotherapeutic resistance and hypoxia-related therapies. Cancer treatment reviews. 2003; 29:297–307. [PubMed: 12927570]
24. Shen J, Xia W, Khotskaya YB, Huo L, Nakanishi K, Lim SO, et al. EGFR modulates microRNA maturation in response to hypoxia through phosphorylation of AGO2. Nature. 2013; 497:383–387. [PubMed: 23636329]
25. Su X, Chakravarti D, Cho MS, Liu L, Gi YJ, Lin YL, et al. TAp63 suppresses metastasis through coordinate regulation of Dicer and miRNAs. Nature. 2010; 467:986–990. [PubMed: 20962848]
26. Tokumaru S, Suzuki M, Yamada H, Nagino M, Takahashi T. let-7 regulates Dicer expression and constitutes a negative feedback loop. Carcinogenesis. 2008; 29:2073–2077. [PubMed: 18700235]
27. van den Beucken T, Koch E, Chu K, Rupaimoole R, Prickaerts P, Adriaens M, et al. Hypoxia promotes stem cell phenotypes and poor prognosis through epigenetic regulation of DICER. Nature communications. 2014; 5:5203.
28. Vaupel P, Mayer A. Hypoxia in cancer: significance and impact on clinical outcome. Cancer metastasis reviews. 2007; 26:225–239. [PubMed: 17440684]
29. Wang X, Zhao X, Gao P, Wu M. c-Myc modulates microRNA processing via the transcriptional regulation of Drosha. Scientific reports. 2013; 3:1942. [PubMed: 23735886]
30. Wu SY, Yang X, Gharpure KM, Hatakeyama H, Egli M, McGuire MH, et al. 2'-OMe-phosphorodithioate-modified siRNAs show increased loading into the RISC complex and enhanced anti-tumour activity. Nature communications. 2014; 5:3459.
31. Yamagishi N, Teshima-Kondo S, Masuda K, Nishida K, Kuwano Y, Dang DT, et al. Chronic inhibition of tumor cell-derived VEGF enhances the malignant phenotype of colorectal cancer cells. BMC cancer. 2013; 13:229. [PubMed: 23651517]

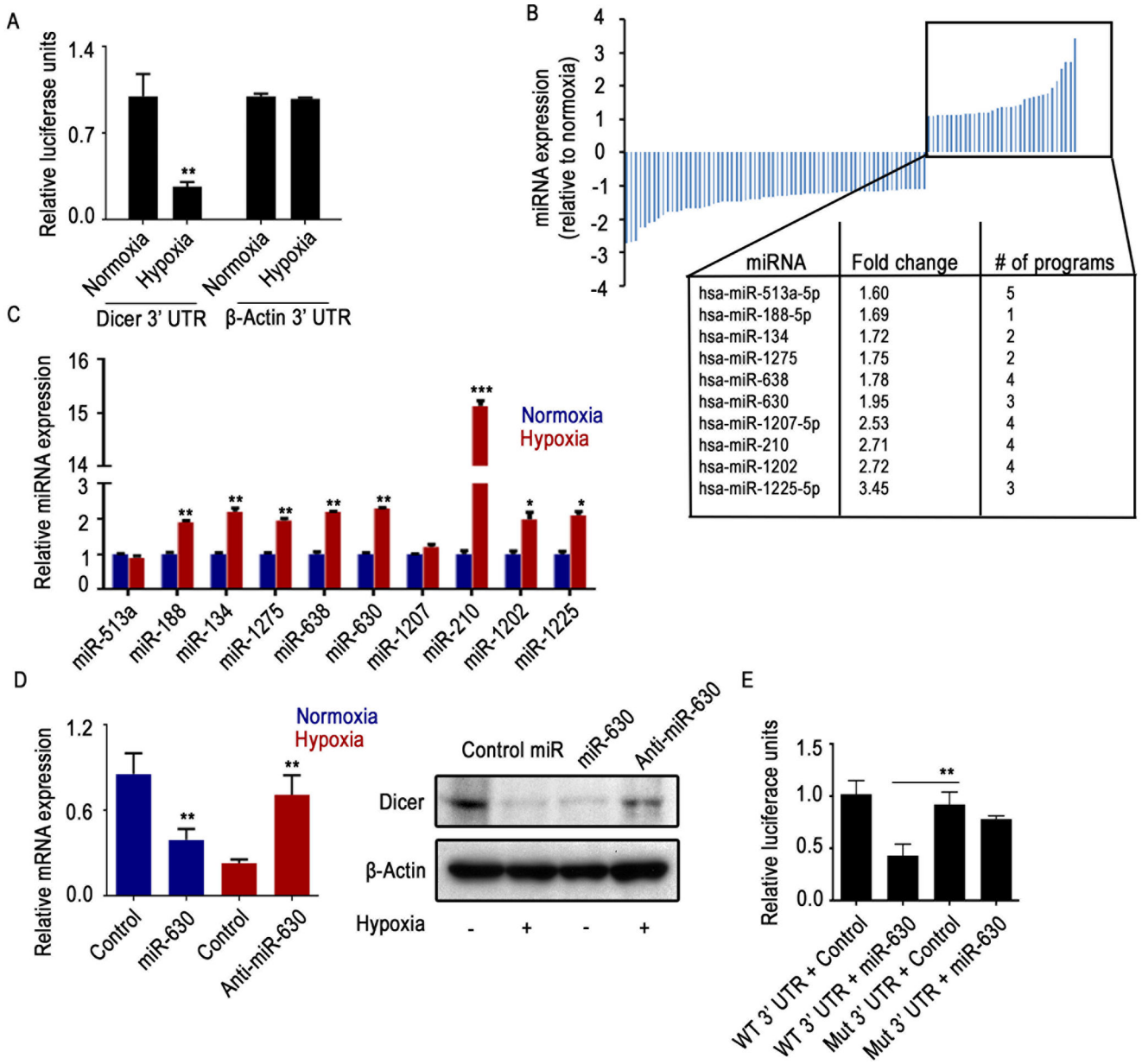

Figure 1. Dicer is downregulated under hypoxic conditions via direct targeting of miR-630

(A) Relative Dicer 3' untranslated region (UTR) and promoter luciferase reporter activity under hypoxic conditions in A2780 cells. β-actin 3'UTR or promoter was used as a control. (B) Expression profiles of significantly deregulated ($p < 0.5$) miRNAs in A2780 cells exposed to hypoxia. MicroRNAs (miRNAs) were profiled using a miRNA microarray of RNA extracted from A2780 cells exposed to hypoxia for 48 hours. The box shows miRNAs upregulated under hypoxic conditions and predicted to target Dicer 3'UTR, with the corresponding fold change and the number of independent software predictions. (C) Levels of mature miRNAs predicted to target Dicer 3'UTR, profiled using quantitative real-time polymerase chain reaction of RNA from A2780 cells exposed to hypoxia for 48 hours. (D) Expression of Dicer in A2780 cells after transfecting the cells with miR-630 under normoxic

conditions or with anti-miR-630 under hypoxic conditions. (E) Dicer 3'UTR wild type (WT) and miR-630 binding site mutant (Mut) luciferase activity in A2780 cells transfected with miR-630 or control miRNA. Data are presented as mean ± standard error of the mean of n ≥ 3 independent experimental groups. *p < 0.05, **p < 0.01, ***p < 0.001 (Student *t* test).

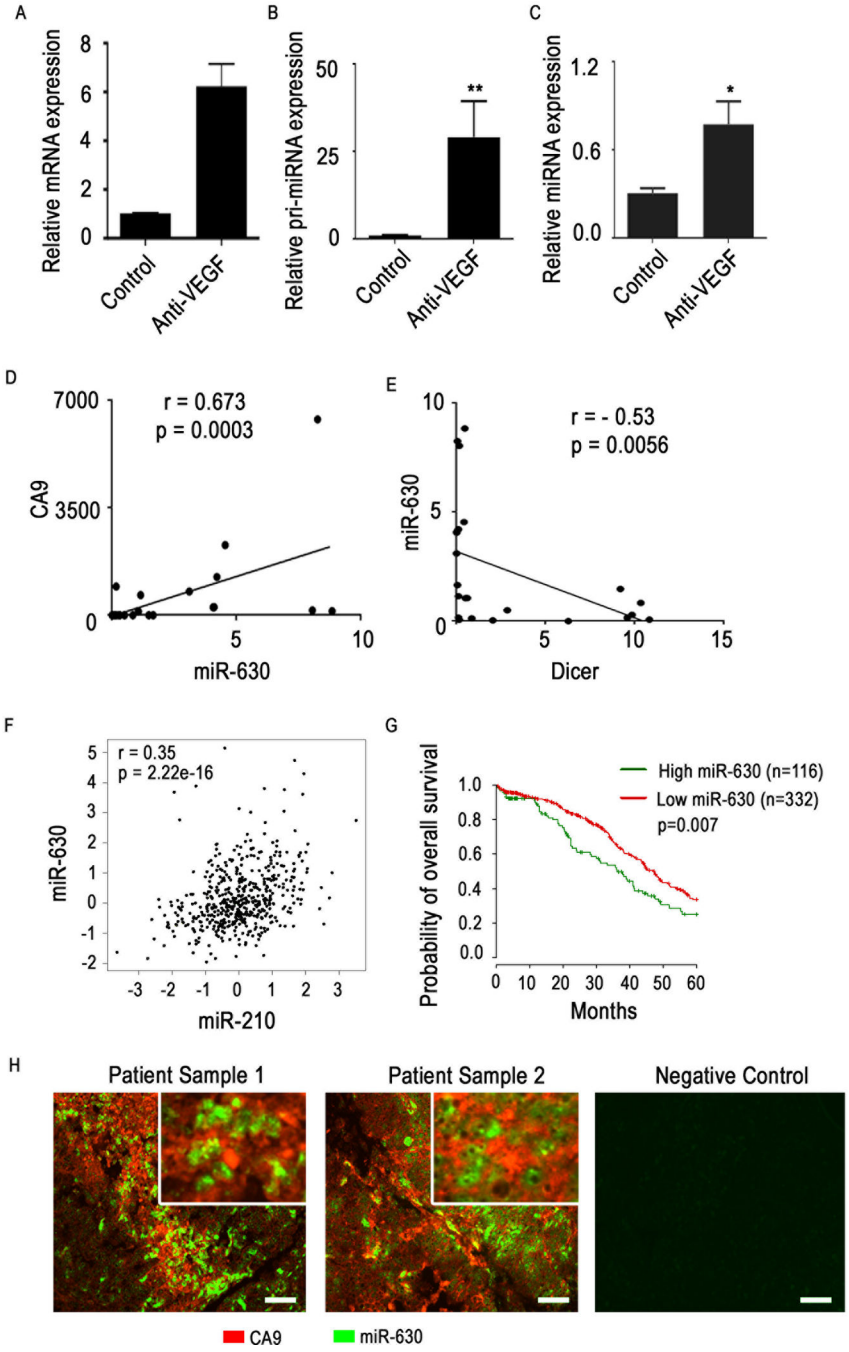

Figure 2. miR-630 expression correlates with hypoxia *in vivo* and in clinical samples of ovarian cancer

(A) Hypoxia marker GLUT1, (B) Precursor and (C) mature miRNA-630 levels in A2780 mouse tumor samples treated with anti-VEGF agent bevacizumab. Pearson correlation graphs comparing (D) hypoxia marker CA9 with miR-630 expression levels and (E) miR-630 with Dicer expression levels in clinical tumor samples (n = 15 with high hypoxia levels and n = 15 with low hypoxia levels). (F) Pearson correlation between miR-630 and hypoxia-upregulated miR-210 in high-grade serous ovarian cancer clinical samples from The Cancer Genome Atlas (TCGA) dataset. (G) Overall disease-specific probability of

survival in patients with high-grade serous ovarian cancer based on tumoral expression of miR-630. Data from the high-grade serous ovarian cancer dataset in TCGA were analyzed. (H) Co-staining of miR-630 and CA9 in tumor samples from patients with ovarian cancer. *In situ* hybridization was used to visualize miR-630 and immunofluorescent staining was used for CA9. Scale bar: 200μm. Data are presented as mean ± standard error of the mean of n ≥ 3 independent experimental groups. *$p < 0.05$, **$p < 0.01$ (Student *t* test).

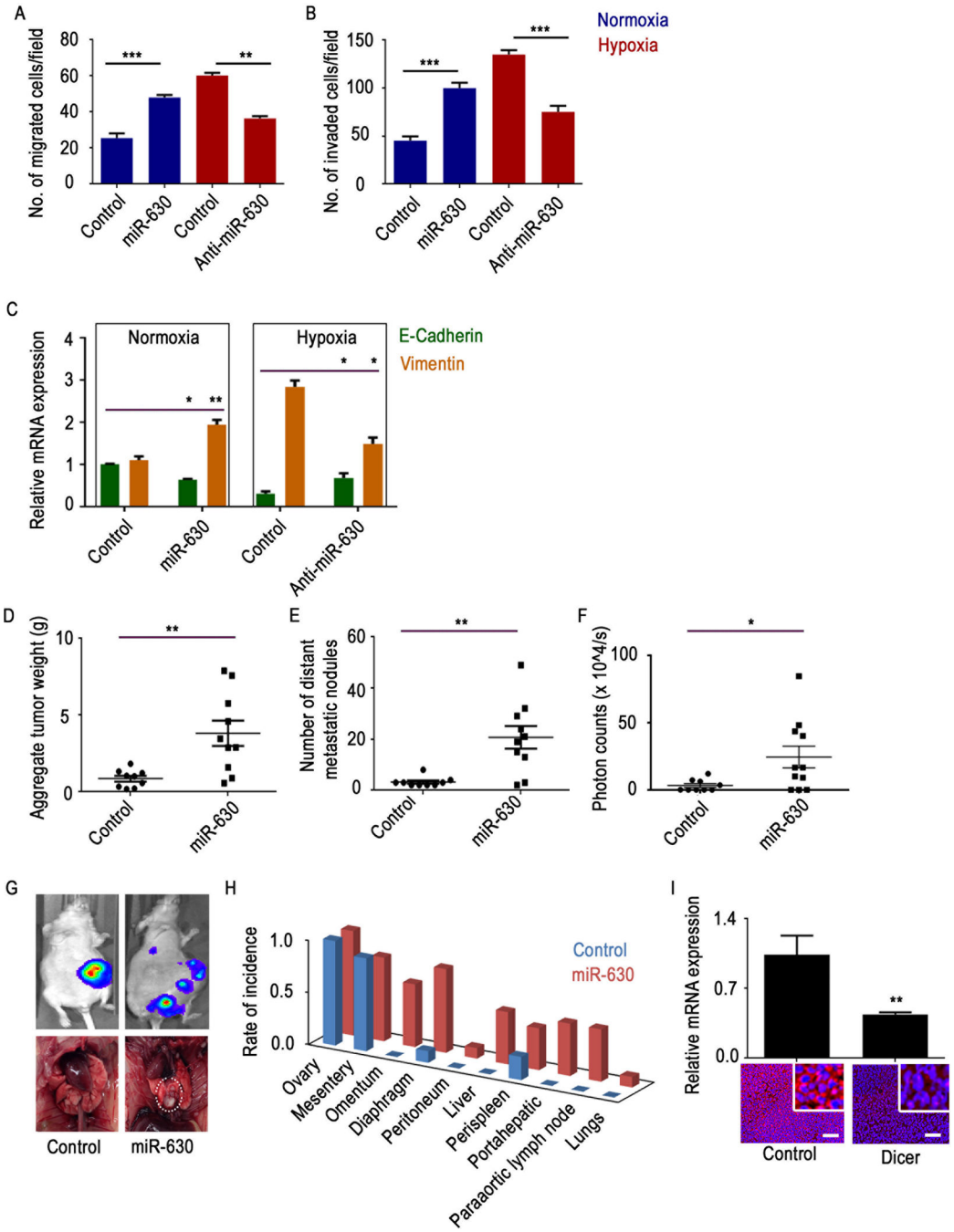

Figure 3. Hypoxia-upregulated miR-630 is involved in increased tumor progression

(A) Migration and (B) invasion of A2780 cancer cells transfected with control microRNA (miRNA) or miR-630 under normoxic conditions or transfected with control mRNA or anti-miR-630 under hypoxic conditions. (C) Expression of epithelial-to-mesenchymal transition markers E-cadherin and vimentin in A2780 cancer cells transfected with control miRNA or miR-630 under normoxic conditions or control miRNA or anti-miR-630 under hypoxic conditions. (D–F) Aggregate tumor mass, number of distant metastatic nodules, and photon counts in A2780 tumors from mice treated with control miRNA or miR-630 (n = 10 mice

per group). (G) Representative luminescence pictures showing tumor burden (top) and photographs of a rare metastatic nodule in the miR-630 group (bottom). (H) Pattern of metastatic spread in mice treated with control miRNA or miR-630. (I) mRNA and protein expression levels of Dicer in A2780 tumor samples from mice treated with control miRNA or miR-630. Scale bar: 200μm. Data are presented as mean ± standard error of the mean of n ≥ 3 independent experimental groups. *p < 0.05, **p < 0.01, ***p < 0.001 (Student *t* test).

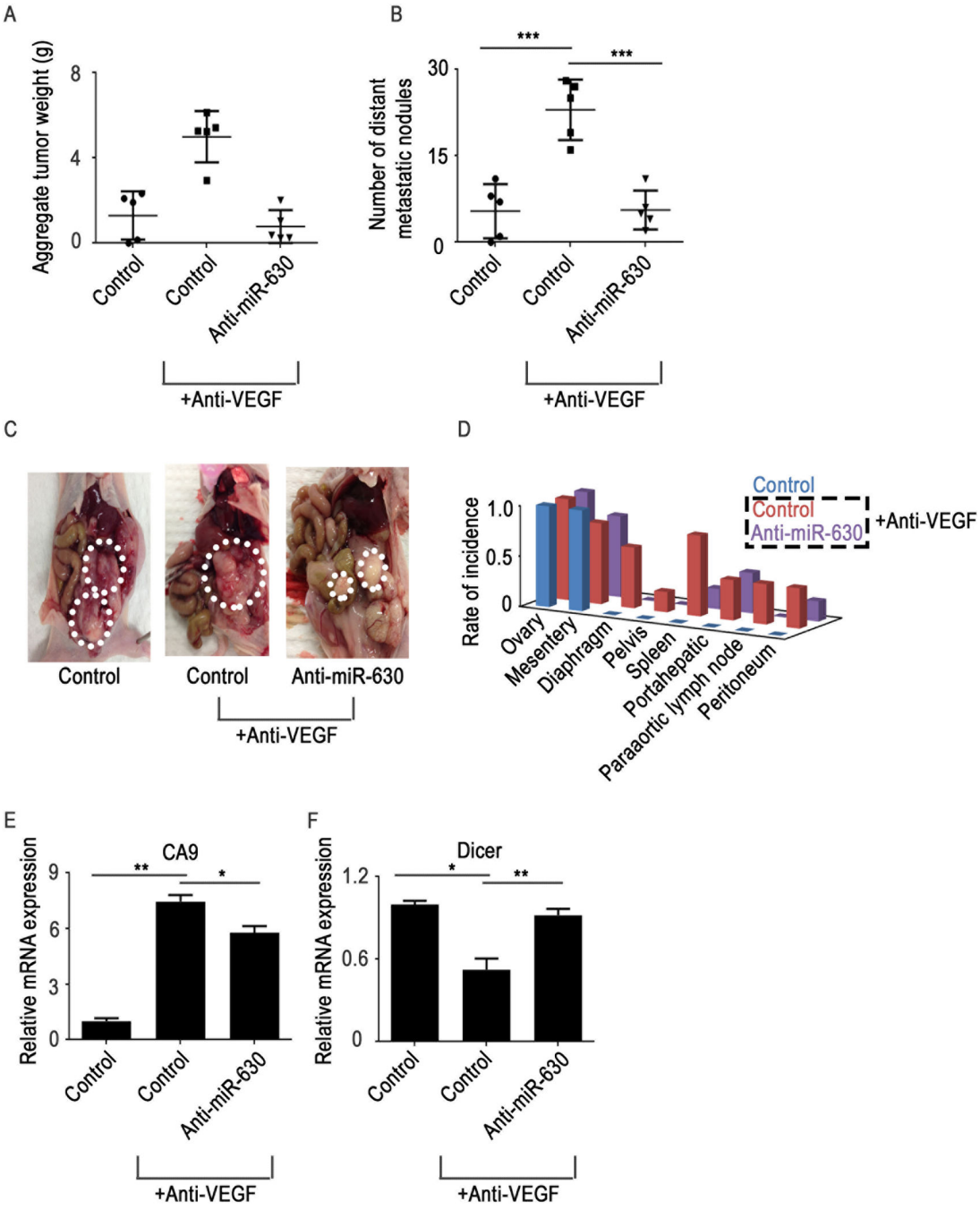

Figure 4. Treatment with the combination of a vascular endothelial growth factor (VEGF) antibody (bevacizumab) and anti-miR-630 results in decreased tumor growth and metastasis

(A–B) Aggregate tumor weight and number of distant metastatic nodules in mice treated with bevacizumab and anti-miR-630 (n = 5 mice per group). (C) Representative pictures of tumor burden in all treatment groups. (D) Distribution of metastatic nodules in all treatment groups. (E–F) Hypoxia marker CA9 and Dicer mRNA expression levels in tumor samples from each treatment group. Data are presented as mean ± standard error of the mean of n ≥ 3 experimental groups. *p < 0.05, **p < 0.01, ***p < 0.001 (Student *t* test).